Polarization properties of surface plasmon enhanced photoluminescence from a single Ag nanowire

Min Song,[1] Gengxu Chen,[1] Yan Liu,[1] E Wu,[1] Botao Wu,[1,2] and Heping Zeng[1,*]

[1] *State Key Laboratory of Precision Spectroscopy, East China Normal University, Shanghai 200062, China*
[2]*btwu@phy.ecnu.edu.cn*
[*]*hpzeng@phy.ecnu.edu.cn*

Abstract: Metallic nanowires are of great research interest due to their applications in surface plasmon polariton coupling of light. The efficiency is much dependent on the polarization of the light due to the phase matching requirement in the light-surface plasmon polariton coupling. By scanning confocal microscope, the photoluminescence from a single Ag nanowire was demonstrated strongly dependent on the excitation laser polarization, showing good consistency with the theoretical simulation. Meanwhile strong avalanche photoluminescence from a single Ag nanowire was observed when the excitation laser was polarized along the long axis of the Ag nanowire. The photoluminescence emission exhibited a polarization-sensitive spatial distribution. This may stimulate promising applications in designing polarization-controllable nanoscale plasmonic devices.

OCIS codes: (160.4236) Nanomaterials; (240.6680) Surface plasmons; (260.5430) Polarization; (250.5230) Photoluminescence.

References and links

1. R. M. Dickson and L. A. Lyon, "Unidirectional plasmon propagation in metallic nanowires," J. Phys. Chem. B **104**(26), 6095–6098 (2000).
2. H. Ditlbacher, A. Hohenau, D. Wagner, U. Kreibig, M. Rogers, F. Hofer, F. R. Aussenegg, and J. R. Krenn, "Silver nanowires as surface plasmon resonators," Phys. Rev. Lett. **95**(25), 257403 (2005).
3. A. W. Sanders, D. A. Routenberg, B. J. Wiley, Y. N. Xia, E. R. Dufresne, and M. A. Reed, "Observation of plasmon propagation, redirection, and fan-out in silver nanowires," Nano Lett. **6**(8), 1822–1826 (2006).
4. S. Lal, S. Link, and N. J. Halas, "Nano-optics from sensing to waveguiding," Nat. Photonics **1**(11), 641–648 (2007).
5. R. F. Oulton, V. J. Sorger, D. A. Genov, D. F. P. Pile, and X. Zhang, "A hybrid plasmonic waveguide for subwavelength confinement and long-range propagation," Nat. Photonics **2**(8), 496–500 (2008).
6. Z. P. Li, F. Hao, Y. Z. Huang, Y. R. Fang, P. Nordlander, and H. X. Xu, "Directional light emission from propagating surface plasmons of silver nanowires," Nano Lett. **9**(12), 4383–4386 (2009).
7. D. Solis, Jr., W. S. Chang, B. P. Khanal, K. Bao, P. Nordlander, E. R. Zubarev, and S. Link, "Bleach-imaged plasmon propagation (BlIPP) in single gold nanowires," Nano Lett. **10**(9), 3482–3485 (2010).
8. W. H. Wang, Q. Yang, F. G. Fan, H. X. Xu, and Z. L. Wang, "Light propagation in curved silver nanowire plasmonic waveguides," Nano Lett. **11**(4), 1603–1608 (2011).
9. H. R. Raether, *Surface Plasmon* (Springer-Verlag, 1988).
10. W. L. Barnes, A. Dereux, and T. W. Ebbesen, "Surface plasmon subwavelength optics," Nature **424**(6950), 824–830 (2003).
11. A. Manjavacas and F. J. García de Abajo, "Robust plasmon waveguides in strongly interacting nanowire arrays," Nano Lett. **9**(4), 1285–1289 (2009).
12. Y. G. Ma, X. Y. Li, H. K. Yu, L. M. Tong, Y. Gu, and Q. H. Gong, "Direct measurement of propagation losses in silver nanowires," Opt. Lett. **35**(8), 1160–1162 (2010).
13. B. Wild, L. Cao, Y. G. Sun, B. P. Khanal, E. R. Zubarev, S. K. Gray, N. F. Scherer, and M. Pelton, "Propagation lengths and group velocities of plasmons in chemically synthesized gold and silver nanowires," ACS Nano **6**(1), 472–482 (2012).
14. P. Kusar, C. Gruber, A. Hohenau, and J. R. Krenn, "Measurement and reduction of damping in plasmonic nanowires," Nano Lett. **12**(2), 661–665 (2012).

#173261 - $15.00 USD Received 25 Jul 2012; revised 10 Sep 2012; accepted 10 Sep 2012; published 14 Sep 2012

15. M. W. Knight, N. K. Grady, R. Bardhan, F. Hao, P. Nordlander, and N. J. Halas, "Nanoparticle-mediated coupling of light into a nanowire," Nano Lett. **7**(8), 2346–2350 (2007).
16. X. Guo, M. Qiu, J. M. Bao, B. J. Wiley, Q. Yang, X. N. Zhang, Y. G. Ma, H. K. Yu, and L. M. Tong, "Direct coupling of plasmonic and photonic nanowires for hybrid nanophotonic components and circuits," Nano Lett. **9**(12), 4515–4519 (2009).
17. Z. P. Li, K. Bao, Y. R. Fang, Y. Z. Huang, P. Nordlander, and H. X. Xu, "Correlation between Incident and emission polarization in nanowire surface plasmon waveguides," Nano Lett. **10**(5), 1831–1835 (2010).
18. R. X. Yan, P. Pausauskie, J. X. Huang, and P. D. Yang, "Direct photonic-plasmonic coupling and routing in single nanowires," Proc. Natl. Acad. Sci. U.S.A. **106**(50), 21045–21050 (2009).
19. Y. R. Fang, Z. P. Li, Y. Z. Huang, S. P. Zhang, P. Nordlander, N. J. Halas, and H. X. Xu, "Branched silver nanowires as controllable plasmon routers," Nano Lett. **10**(5), 1950–1954 (2010).
20. Y. R. Fang, H. Wei, F. Hao, P. Nordlander, and H. X. Xu, "Remote-excitation surface-enhanced Raman scattering using propagating Ag nanowire plasmons," Nano Lett. **9**(5), 2049–2053 (2009).
21. C. L. Du, Y. M. You, T. Chen, Y. Zhu, H. L. Hu, D. N. Shi, H. Y. Chen, and Z. X. Shen, "Individual Ag nanowire dimer for surface-enhanced Raman scattering," Plasmonics **6**(4), 761–766 (2011).
22. A. V. Akimov, A. Mukherjee, C. L. Yu, D. E. Chang, A. S. Zibrov, P. R. Hemmer, H. Park, and M. D. Lukin, "Generation of single optical plasmons in metallic nanowires coupled to quantum dots," Nature **450**(7168), 402–406 (2007).
23. H. Wei, D. Ratchford, X. E. Li, H. Xu, and C. K. Shih, "Propagating surface plasmon induced photon emission from quantum dots," Nano Lett. **9**(12), 4168–4171 (2009).
24. R. Kolesov, B. Grotz, G. Balasubramanian, R. J. Stöhr, A. A. L. Nicolet, P. R. Hemmer, F. Jelezko, and J. Wrachtrup, "Wave-particle duality of single surface plasmon polaritons," Nat. Phys. **5**(7), 470–474 (2009).
25. J. H. Li and R. Yu, "Single-plasmon scattering grating using nanowire surface plasmon coupled to nanodiamond nitrogen-vacancy center," Opt. Express **19**(21), 20991–21002 (2011).
26. E. Ozbay, "Plasmonics: merging photonics and electronics at nanoscale dimensions," Science **311**(5758), 189–193 (2006).
27. K. Leosson, T. Nikolajsen, A. Boltasseva, and S. I. Bozhevolnyi, "Long-range surface plasmon polariton nanowire waveguides for device applications," Opt. Express **14**(1), 314–319 (2006).
28. J. J. Ju, S. Park, M. S. Kim, J. T. Kim, S. K. Park, Y. J. Park, and M. H. Lee, "40 Gbit/s light signal transmission in long-range surface plasmon waveguides," Appl. Phys. Lett. **91**(17), 171117 (2007).
29. P. Neutens, P. Van Dorpe, I. De Vlaminck, L. Lagae, and G. Borghs, "Electrical detection of confined gap plasmons in metal–insulator–metal waveguides," Nat. Photonics **3**(5), 283–286 (2009).
30. Y. Li, F. Qian, J. Xiang, and C. M. Lieber, "Naowires electronic and optoelectronic devices," Mater. Today **9**(10), 18–27 (2006).
31. D. Ugarte, A. Chatelain, and W. A. de Heer,"Nanocapillarity and chemistry in carbon nanotubes," Science **274**(5294), 1897–1899 (1996).
32. E. Braun, Y. Eichen, U. Sivan, and G. Ben-Yoseph, "DNA-templated assembly and electrode attachment of a conducting silver wire," Nature **391**(6669), 775–778 (1998).
33. T. D. Lazzara, G. R. Bourret, R. B. Lennox, and T. G. M. van de Ven, "Polymer templated synthesis of AgCN and Ag nanowires," Chem. Mater. **21**(10), 2020–2026 (2009).
34. R. L. Zong, J. Zhou, Q. Li, B. Du, B. Li, M. Fu, X. W. Qi, L. T. Li, and S. Buddhudu, "Synthesis and optical properties of silver nanowire arrays embedded in anodic alumina membrane," J. Phys. Chem. B **108**(43), 16713–16716 (2004).
35. Y. G. Sun, B. Mayers, T. Herricks, and Y. N. Xia, "Polyol synthesis of uniform silver nanowires: a plausible growth mechanism and the supporting evidence," Nano Lett. **3**(7), 955–960 (2003).
36. K. E. Korte, S. E. Skrabalak, and Y. N. Xia, "Rapid synthesis of silver nanowires through a CuCl- or $CuCl_2$-mediated polyol process," J. Mater. Chem. **18**(4), 437–441 (2008).
37. C. Wang, Y. J. Hu, C. M. Lieber, and S. H. Sun, "Ultrathin Au nanowires and their transport properties," J. Am. Chem. Soc. **130**(28), 8902–8903 (2008).
38. F. Kim, K. Sohn, J. S. Wu, and J. X. Huang, "Chemical synthesis of gold nanowires in acidic solutions," J. Am. Chem. Soc. **130**(44), 14442–14443 (2008).
39. X. X. Li, L. Wang, and G. Q. Yan, "Review: recent research progress on preparation of silver nanowires by soft solution methods and their applications," Cryst. Res. Technol. **46**(5), 427–438 (2011).
40. L. A. Peyser, A. E. Vinson, A. P. Bartko, and R. M. Dickson, "Photoactivated fluorescence from individual silver nanoclusters," Science **291**(5501), 103–106 (2001).
41. K. Ueno, S. Juodkazis, V. Mizeikis, K. Sasaki, and H. Misawa, "Clusters of closely spaced gold nanoparticles as a source of two-photon photoluminescence at visible wavelengths," Adv. Mater. (Deerfield Beach Fla.) **20**(1), 26–30 (2008).
42. E. Wu, Y. Z. Chi, B. T. Wu, K. W. Xia, Y. Yokota, K. Ueno, H. Misawa, and H. P. Zeng, "Spatial polarization sensitivity of single Au bowtie nanostructure," J. Lumin. **131**(9), 1971–1974 (2011).
43. H. M. Gong, Z. K. Zhou, S. Xiao, X. R. Su, and Q. Q. Wang, "Strong near-infrared avalanche photoluminescence from Ag nanowire arrays," Plasmonics **3**(2–3), 59–64 (2008).
44. R. Sarkar, P. Kumbhakar, A. K. Mitra, and R. A. Ganeev, "Synthesis and photoluminescence properties of silver nanowires," Curr. Appl. Phys. **10**(3), 853–857 (2010).

#173261 - $15.00 USD Received 25 Jul 2012; revised 10 Sep 2012; accepted 10 Sep 2012; published 14 Sep 2012

45. D. A. Clayton, D. M. Benoist, Y. Zhu, and S. L. Pan, "Photoluminescence and spectroelectrochemistry of single ag nanowires," ACS Nano **4**(4), 2363–2373 (2010).
46. J. J. Mock, S. J. Oldenburg, D. S. Smith, D. A. Schultz, and S. Schultz, "Composite plasmon resonant nanowires," Nano Lett. **2**(5), 465–469 (2002).
47. G. Schider, J. R. Krenn, A. Hohenau, H. Ditlbacher, A. Leitner, F. R. Aussenegg, W. L. Schaich, I. Puscasu, B. Monacelli, and G. Boreman, "Plasmon dispersion relation of Au and Ag nanowires," Phys. Rev. B **68**(15), 155427 (2003).
48. Q. Q. Wang, J. B. Han, D. L. Guo, S. Xiao, Y. B. Han, H. M. Gong, and X. W. Zou, "Highly efficient avalanche multiphoton luminescence from coupled Au nanowires in the visible region," Nano Lett. **7**(3), 723–728 (2007).

1. Introduction

One-dimensional metallic Ag or Au nanowires (NWs) can be used to guide photons at visible and near-infrared range by coupling electromagnetic wave to collective electron oscillation on their surface which is known as surface plasmon polariton (SPP) [1–8]. Plasmonic metallic NWs serve as waveguides for plasmon propagation, provide the possibility to break the diffraction limit and localize the electromagnetic energy to scales less than $\lambda/10$ [9,10], which have been thoroughly investigated in recent studies reporting on SPP propagation [1–3,5,8], SPP damping along NWs [7,11–14], the coupling and splitting of SPP with light [15–19], surface enhanced Raman scattering [20,21], and the interaction of SPP with single-photon emitters such as quantum dots [22,23] or color centers in nanodiamonds [24,25]. Furthermore, plasmonic NWs provide an appealing nanophotonic platform for miniaturization of optical signal processing and sensing devices at subwavelength scale and integration of photonic circuits with external devices to overcome the fundamental data transmission rates and bandwidth limitations in conventional electrical technology [26–30].

Generally, metallic NWs are synthesized by two methods: template-directed approaches [31–34] and chemical synthesis [35–39]. The plasmons supported by the metallic nanowires fabricated by templates usually suffer large losses due to scattering from the grain boundaries and rough surfaces of NWs [2]. On the other hand, chemical synthesis has been demonstrated as a simple and inexpensive route for the bottom-up preparation of metallic NWs with very smooth surfaces and without grain boundaries [35–39]. Chemically grown Au NWs have in principle the same advantages as Ag NWs, but Au is intrinsically lossier, especially at optical frequencies. Thus, the studies about plasmonic activities and synthetic work of Ag NWs are always flourishing [1–39]. It is known that Ag or Au nanostructures can emit strong fluorescence under visible light excitation, which is believed as a result of radiative recombination of Fermi level electrons and sp- or d-band holes [40–42]. As for Ag NWs, near-infrared and visible photoluminescence (PL) from Ag NW arrays and assembles has been observed under visible laser excitation [43,44]. However, there were few reports on the PL from single Ag NWs [45]. More importantly, as one kind of one-dimentional nanostructure, the polarization properties of PL from a single Ag NW has not been studied in detail.

In this letter, PL properties from a single Ag NW with the diameter about 130 nm and perfect surface quality were studied under excitation at 532 nm. The PL intensity from a single Ag NW showed strong dependence on the polarization direction of the excitation laser. Furthermore, the excitation power dependence and emission polarization properties of the PL from a single Ag NW were investigated. An elongated single Ag NW emitted a strong avalanche PL under excitation polarized along its long axis, suggesting strong surface plasmon coupling effect between light and resonant free electrons in the NW surface. The PL emission was revealed to exhibit a polarization-sensitive spatial distribution.

2. Experimental section

The Ag NWs were synthesized as described in detail as following. 5 mL of ethylene glycol (EG) were stirred in a glass vial, suspended in an oil bath (150 °C). After the EG was heated for 1 h under stirring, 40μ L of a 4 mM copper(II) chloride ($CuCl_2$) solution in EG was

#173261 - $15.00 USD Received 25 Jul 2012; revised 10 Sep 2012; accepted 10 Sep 2012; published 14 Sep 2012

injected into the heated EG. After an additional 15 min, 1.5 mL of a 0.094 M $AgNO_3$ solution in EG was injected into the hot solution followed immediately by 1.5 mL of a 0.147 M PVP (molecular weight $M_w \approx 55000$, concentration expressed in terms of monomer) solution in EG added dropwise over a period of 2 min. The reaction was continued at 150 °C for another 1 h and quenched in water. The reaction products were washed with acetone, collected by centrifugation at about 2000 rpm for 20 min, and then washed with ethanol for three times, finally dispersed in ethanol for further use. The morphology and size of the obtained Ag NWs were characterized by a scanning electron microscopy (SEM) (JEOL JSM-5610LV), and optical absorption spectra were measured using a UV-Vis-NIR spectrophotometer (JASCO V-570). Samples for the PL measurement of single Ag NW were prepared by spin-coating the dilute suspension of Ag NWs in ethanol on clean glass substrates, and then coated immediately with polymethyl methacrylate (PMMA) thin films of about 40 nm thickness by spin-coating method to avoid the oxidation of Ag NWs in air.

Using a home-made scanning confocal microscope system, spatial polarization properties of the PL from a single Ag NW were investigated. A 532 nm solid-state laser (continuous wave) was used as the excitation source. A polarizer was added at the output of the laser to force a linear polarization and the polarization direction was tuned by the half-wave-plate behind the polarizer before the microscope objective. The laser beam was focused into diffraction-limited spot on one end of a single Ag NW by a high numerical aperture microscope objective (NA = 0.95, × 100). PL from a single Ag NW was collected by the same microscope objective, sent to the detector after spatial and spectral filtering, and then detected by a silicon avalanche photodiode (APD). To measure of emission polarization contrast, a half-wave-plate and a polarizer were placed before the detector. By rotating the half-wave-plate in front of the detector the polarization of PL emitted from the single Ag NW could be checked.

3. Results and discussion

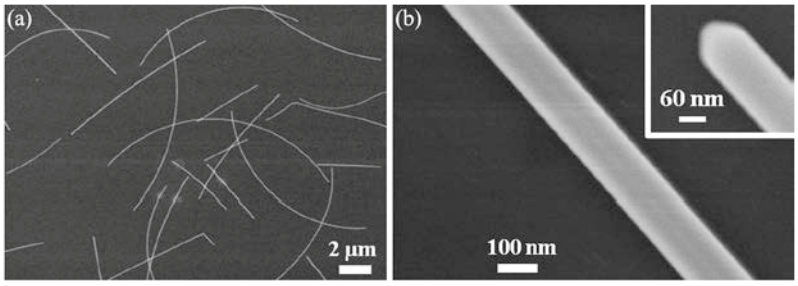

Fig. 1. (a) SEM image of Ag NW assembles synthesized by polyol reduction of $AgNO_3$. (b) SEM image of single Ag NW, revealing the very smooth surface. Inset: an SEM image of one end of Ag NW.

Figure 1(a) shows a typical SEM image of fabricated Ag NWs on a silicon wafer. Ag NWs could be well dispersed with a low density and spin-coated on the substrates, which facilitated the measurement of PL from a single Ag NW. As shown in Fig. 1(a), the length of Ag NWs varied from few to tens of micrometers. On the other hand, in the enlarged SEM image of Fig. 1(b), the NWs exhibited a very smooth surface and were quite uniform in their dimensions with an average diameter of ~130 nm. The end of the individual Ag NW exhibited a pyramid structure as shown in the inset of Fig. 1(b), showing that the silver NWs were grown from seeds deriving from twinned bicrystalline particles of decahedral shape [35].

Surface plasmon resonance property of Ag NWs was characterized in Fig. 2. The dilute suspension of Ag NWs in ethanol was held in a quartz cell of path length 1 cm and the spectrum was recorded by a UV-Vis-NIR spectrophotometer. Two extinction peaks around 350 and 395 nm could be observed, which corresponds to the quadruple resonance excitation

#173261 - $15.00 USD Received 25 Jul 2012; revised 10 Sep 2012; accepted 10 Sep 2012; published 14 Sep 2012

and transverse surface plasmon resonance (TSPR) of Ag NWs, respectively [46]. We observed no extinction peaks from the longitudinal surface plasmon resonance (LSPR) of Ag NWs up to 2.5 μm. Since the aspect ratio of the Ag nanowires was sufficiently large, the plasmon resonances associated with the long and short axes are entirely decoupled and accordingly, the peaks corresponding to LSPR of nanowires disappeared [47].

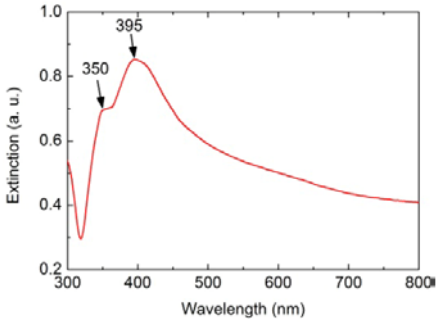

Fig. 2. Extinction spectrum of Ag NWs in ethanol solution.

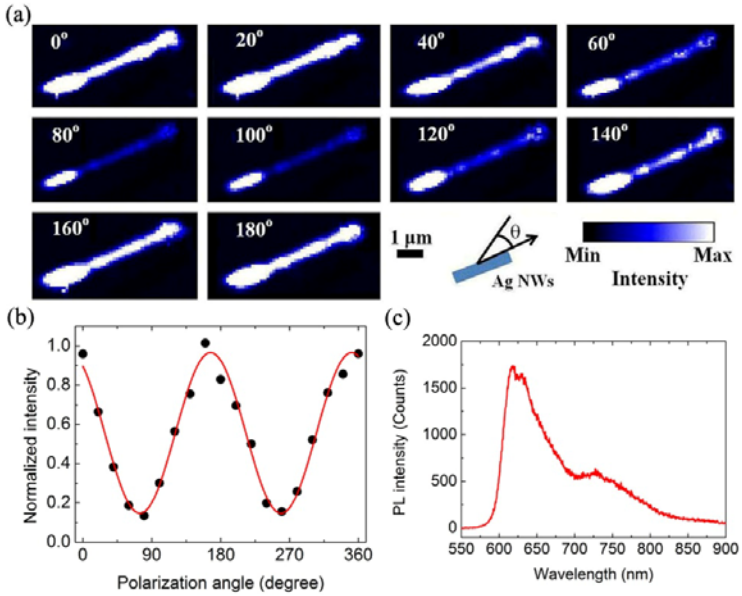

Fig. 3. (a) PL scan image of a single Ag NW dependent on the polarization angle of the excitation laser. (b) Normalized PL intensity from a single Ag NW as a function of the excitation laser polarization angle. The solid dots represent the experimental data and the solid line represents a fit based on sinusoid. (c) A typical PL spectrum of a single Ag NW.

The spatial distribution of the PL from a single Ag NW by different excitation laser polarization directions was examined by using a scanning confocal microscope. Figure 3(a) shows the PL images from a single Ag NW. According to the evolution of the PL images with the excitation laser polarization direction, it could be observed that the PL intensity from a single Ag NW exhibited a strong dependence on the excitation laser polarization direction and varied with a period of 180°. Figure 3(b) plots the PL intensity versus the excitation polarization direction related to the long axis of the single Ag NW. The maximum and minimum PL intensity were reached as the excitation laser was polarized parallel and perpendicularly to the long axis of Ag NWs, respectively. The PL intensity contrast was

#173261 - $15.00 USD Received 25 Jul 2012; revised 10 Sep 2012; accepted 10 Sep 2012; published 14 Sep 2012

calculated to be about 85%, showing a large polarization sensitivity of the single Ag NW on the excitation laser polarization. Interestingly, it could also be clearly seen that the PL intensity was not uniformly distributed along the long axis of the Ag NWs as in the SEM image in Fig. 1. This could be explained by the inhomogeneity in the crystal structure at different sites along the NWs as well as the surface adsorption of surfactant PVP used during the process of NW synthesis [45]. A typical PL spectrum of a single Ag NW is shown in Fig. 3(c). The PL spectrum showed a broad peak near 625 nm with a shoulder peak around 725 nm. The whole spectrum ranged from 575 to 850 nm. The similar PL spectra were obtained when measured on the different positions along Ag NW. We also conducted the measurement on the area of the sample without Ag NWs, but no apparent luminescent signal was observed. The measurement on other individual Ag NWs was repeated in the same conditions and similar phenomenon was observed as mentioned above. The large dependence of the PL intensity from a single Ag NW on the excitation laser polarization direction should be related to the distribution of the local electric filed strength on the NWs interacting with the incident optical field.

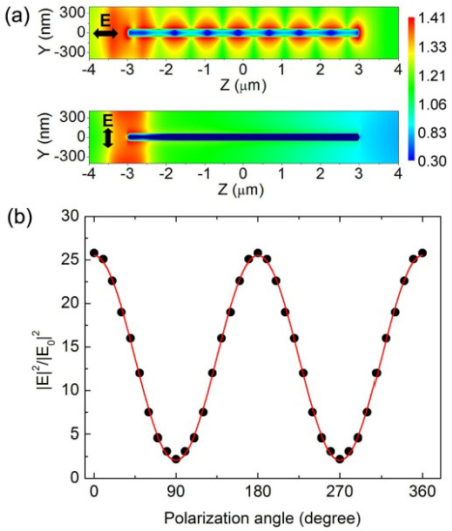

Fig. 4. Polarization dependence of the average electric field intensity enhancement. (a) Electric field intensity contours obtained from the FDTD calculations on a single Ag NW under the parallel and perpendicular excitation polarization relative to the long axis of the Ag NW. The field intensity is at the logarithmic scale. (b) Field intensity enhancement factor (solid circles) as a function of the excitation polarization direction relative to the long axis of the Ag NW. The red line is a sinusoid fit.

FDTD was performed to reveal the local electric field strength contours of a single Ag NW using FDTD Solutions 7.5 (Lumerical Solutions, Inc). The simulation was conducted on a cubic grid with a discretization step of 10 nm with perfectly-matched layer conditions imposed at the boundaries. A plane wave with electric field intensity of E_0 was used to excite one end of a single Ag NW and computed its evolution along the long axis of the Ag NW according to the Maxwell's equations. The Ag NW was considered as a cylinder capped with an oblate spheroid at each end. The diameter of the cylinder was 130 nm, and the length was about 6 μm, which very closed to the footprint size as Ag NW in Fig. 3(a). The semimajor and semiminor axes of the spheroid were 65 and 50 nm, respectively. The Ag NW was placed on a thin substrate with refractive index n = 1.47, matching that of the silica glass substrate used in the experiment. The local electric field enhancement was simulated with different incident light polarization directions. Figure 4(a) shows the average enhancement field contours of the local electric field intensity of a single Ag NW when the incident light was

#173261 - $15.00 USD Received 25 Jul 2012; revised 10 Sep 2012; accepted 10 Sep 2012; published 14 Sep 2012

parallel and perpendicular to the long axis of the Ag NW. For the parallel incident polarization light, the longitudinal SPP mode was excited at the left end of the Ag NW, and propagated along its long axis up to the right end. The radiation recombination transition of electron-hole along the whole NW could be activated and produce strong PL. For the perpendicularly polarized incident light, the transverse SPP mode was excited and only located around the excited end of the Ag NW. Furthermore, the average enhancement factor of the electric field intensity for the parallel incident polarization was about 15 times larger than that for the perpendicular one. Thus, the PL intensity from a single Ag NW excited in the parallel incident light polarization was significantly stronger than that excited in the perpendicular one. Figure 4(b) illustrates the plots of the average enhancement factor of the electric field intensity of a single Ag NW as a function of the incident light polarization. We defined 0° for the incident light polarization direction along the long axis of the Ag NW. As the excitation laser was polarized along (0° or 180°) or perpendicular (90° or 270°) to the long axis of the Ag NW, the largest or smallest average enhancement factor could be achieved, respectively. The experimental results exhibited an excellent agreement with the FDTD simulation on local electric filed enhancement (Figs. 3 and 4).

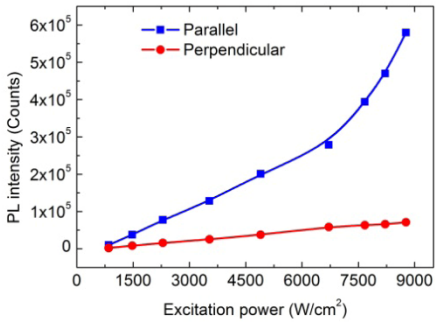

Fig. 5. PL intensity dependence on the excitation laser power in parallel and perpendicular polarization excitation directions.

The PL intensity dependence of a single Ag NW on the excitation light power was examined for parallel and perpendicularly polarized laser excitation, respectively, as shown in Fig. 5. With the increase of the excitation laser power, the PL intensity for the perpendicular incident polarization always increased linearly. On the contrary, the PL intensity excited by parallel polarized laser increased linearly as the laser power was below 6713 W/cm^2 and then increased rapidly at higher powers, showing an avalanche phenomenon. Here, we refer to the avalanche PL as a sudden increase of PL intensity when the laser power is larger than a threshold value. The avalanche PL from a single Ag NW when excited in the parallel incident polarization direction may be related to the strong SPP coupling between light and resonating free electrons in the surface of the Ag NW. The similar avalanche PL has also been observed in Au and Ag NWs arrays under pulse laser excitation [43,48], however, the physics mechanism under them was still not clear. One possible explanation was that the strong field enhancement induced by the resonance coupling of light and surface free electrons in NWs greatly increased the probability to excite the electrons to higher levels by multiphoton absorption and/or multiple excitation and thus led to the avalanche PL [48]. As for our case, the avalanche PL was generated by the continuous wave laser excitation, and the detailed mechanism of avalanche PL need to be further studied. Now the related experiments are conducting in order to uncover the mechanism of the avalanche PL from a single Ag NW.

A half-wave plate and a polarizer were added before the detector to analysis the polarization state of the PL under different excitation polarizations. In order to distinguish the influence of excitation laser polarization direction to the polarization contrast of the PL, the PL intensity under the parallel and perpendicular polarization direction of the incident light

#173261 - $15.00 USD Received 25 Jul 2012; revised 10 Sep 2012; accepted 10 Sep 2012; published 14 Sep 2012

was measured separately and the PL intensity as a function of the polarization angle relative to the long axis of the Ag NW is displayed in Fig. 6. It could be observed that, for either parallel or perpendicularly polarized excitation, the strongest (or weakest) PL intensity was always observed in the parallel (or vertical) polarization direction with the excitation laser, which could be explained that the longitudinal (or transverse) SPP mode was mainly excited in the parallel (or vertical) polarization laser direction. The PL intensity variation was dependent on the polarization direction of the excitation laser linearly. The PL polarization feature could be characterized by the polarization contrast P as

$$P = \frac{I_{\parallel} - I_{\perp}}{I_{\parallel} + I_{\perp}} \tag{1}$$

where I_{Π} and $I_{\perp}$ are the PL intensity under the parallel and vertical directions related to the polarization directions of the excitation laser, respectively. According to the experimental data shown in Fig. 6, the polarization contrast for the parallel and perpendicular polarized incident light was about 0.88 and 0.70, respectively. This indicates that the PL intensity from a single Ag NW is spatially more polarized when the incident polarization is along the long axis of the Ag NW.

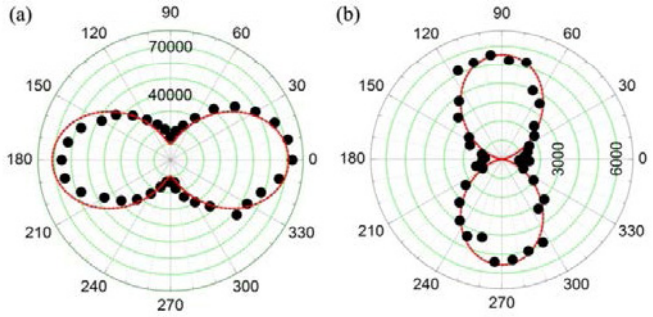

Fig. 6. The PL emission polarization from a single Ag NW under different excitation laser polarization directions: (a) parallel and (b) perpendicular. The red solid curves are a fit.

4. Conclusion

In summary, we have observed that the PL from a single Ag NW was very sensitive to the polarization direction of incident excitation light and varied with a period of 180°, which was in good agreement with the results of FDTD simulation. Strong avalanche PL from a single Ag NW was found when the polarization direction of incident light was along the length axis of single Ag NW due to strong surface plasmon coupling effect. The emission polarization investigation indicated that the spatial distribution of the PL intensity was polarization sensitive. The polarization feature of the PL from a single Ag NW plasmonic waveguide may be useful in applications of nanophotonics, polarization-dependent image, sensing and biolabeling.

Acknowledgments

This work was funded in part by the National Nature Science Fund (11104079, 10990101, 61127014, and 91021014), International Cooperation Projects from Ministry of Science and Technology (2010DFA04410), the Research Fund for the Doctoral Program of Higher Education of China (20110076120019), and the Program of Introducing Talents of Discipline to Universities (B12024).

#173261 - $15.00 USD Received 25 Jul 2012; revised 10 Sep 2012; accepted 10 Sep 2012; published 14 Sep 2012